

# Magneto-optical investigations of LZO buffer layer thickness effects on YBCO microstructure in the simple NiW/LZO/YBCO structure

T. Caroff, L. Porcar, P. Chaudouët, A. Abrutis, C. Jiménez, P. Odier and F. Weiss

**Abstract**— The  $\text{Ni}_{\text{RABiTS}}/\text{La}_2\text{Zr}_2\text{O}_7\text{MOD}/\text{YBa}_2\text{Cu}_3\text{O}_{7\text{MOCVD}}$  structure is a promising architecture for (YBCO) coated conductors. We succeeded in growing highly textured superconducting YBCO films on LZO-buffered Ni-5at%W (NiW) substrates by metalorganic chemical vapor deposition (MOCVD). A single LZO buffer layer grown by metalorganic decomposition (MOD) is sufficient to ensure structural compatibility between YBCO and Ni, and to protect the substrate from oxidation during YBCO deposition. Textured Ni substrates obtained by rolling technique have intrinsic defects such as grain boundaries and rolling scratches. It is not easy to highlight their effects on LZO and YBCO films by usual measurements like XRD or SEM. The combination of Electron Backscattered Diffraction (EBSD) and Magneto-Optics imaging (MO) is useful to image grain boundaries and flux distribution in coated conductors. It provides complementary information on superconducting film qualities. These two techniques allowed us to understand how the microstructure of the LZO buffer layer and thus of the YBCO film is linked to the current density in this simple heterostructure.

**Index Terms**— Coated conductors, Magneto-optical imaging, EBSD, microstructure

## I. INTRODUCTION

Magneto-optical imaging (MO) is a useful tool to study superconducting properties of thin film materials with a spatial resolution of a few micrometers [1-3]. This technique makes possible to detect defects in superconducting layers. The MO is based on Faraday effect, which is the rotation of polarized light under an applied magnetic field ( $\mu_0 * H_{\text{ext}}$ ) [4]. Recently XRD analysis and MO observations were performed

on the new architecture NiW/LZO/YBCO, which is an interesting solution for coated conductors (CCs) [5].

These CCs, processed by all-chemical routes, are based on the excellent quality of lanthanum zirconate,  $\text{La}_2\text{Zr}_2\text{O}_7$  (LZO), used as a buffer layer. Metal organic decomposition (MOD) allows growing LZO on Ni-based substrates in reducing atmosphere, which avoids the undesirable oxidation of the substrate. Pyrochlore LZO (Fd3m) lattice parameters match these of YBCO ( $|( \epsilon_{\text{YBCO}} - \epsilon_{\text{LZO}} ) / \epsilon_{\text{LZO}} | = 1.05\%$ ) and provides a good barrier against  $\text{O}_2$  diffusion [6]. This material fills all the requirements for buffer layers (structural and chemical compatibility between substrate and active layer) and has been used as a single buffer layer in the simple NiW/LZO/YBCO architecture. Even if this architecture is simple, it provides good current transport properties:  $J_c = 0.8 \text{ MA}\cdot\text{cm}^{-2}$  and  $I_c/w = 34 \text{ A/cm}$  on a 700 nm thick YBCO film. We noticed that  $J_c$  increases with LZO thickness, and we aimed to learn more about this important result.

In this paper we present XRD, EBSD and MO investigations on YBCO films deposited on different LZO thicknesses (from 60 to 250 nm) to understand why higher  $J_c$  of YBCO layer is observed for thicker LZO layers.

## II. EXPERIMENTAL

Biaxially textured NiW RABiTS (Rolling Biaxially Textured Substrates) presenting a cubic texture were provided by Evico GmbH (Dresden) and described previously [7]. The grain size of the substrate is around 50  $\mu\text{m}$  and its thickness is 150  $\mu\text{m}$ . Despite grains boundaries and rolling scratches, RABiTS tapes present a small roughness (mean square roughness,  $R_{\text{rms}} < 5 \text{ nm}$ ). Lanthanum zirconate (LZO) was grown on NiW and  $\text{LaAlO}_3$  (LAO) substrates by MOD according to a procedure previously described [5, 8]. LZO layers were deposited with a thickness ranging from 70 nm to 250 nm. LZO thicknesses were evaluated by IR-reflectometry. YBCO films were deposited by pulsed injection MOCVD on the LZO buffered Ni tape according to a procedure described in [5]. The transport properties of the Ni/LZO/YBCO layers were evaluated by  $J_c$  3<sup>rd</sup> harmonic measurements method and compared to values obtained with YBCO films deposited on LAO in the same conditions.

Manuscript received 19 August 2008. This work was supported by the Région Rhône-Alpes SESUC and ANR MADISUP projects, France. We acknowledge M. Decroux (Department of Condensed Matter Physics of Geneva University) for the  $J_c$  third harmonic measurements.

T. Caroff, P. Chaudouët, C. Jimenez and F. Weiss are with Laboratoire des Matériaux et du Génie Physique–CNRS UMR 5628 INP Grenoble Minatec, 3 parvis Louis Néel, BP 257, F-38016 Grenoble, France (corresponding author to provide phone: 00 33 (0)4 76 88 90 32; fax: 00 33 (0)4 76 88 12 80; e-mail: laureline.porcar@grenoble.cnrs.fr).

T. Caroff, L. Porcar and P. Odier are with Institut Néel–CRETA CNRS UPS 2070-25, Avenue des martyrs, BP 166, F-38042 Grenoble, France

A. Abrutis is with the Department of General and Inorganic Chemistry, Vilnius University, Naugarduko Street 24, LT-03225 Vilnius, Lithuania

Film texture and epitaxial relations among the different layers were determined by X-Ray Diffraction (XRD) in Shultz geometry using a D5000 Siemens four-circle diffractometer with monochromatic Cu K $\alpha$  radiation ( $\lambda = 0.15418$  nm), and orientation maps were performed by Electron Backscattered Diffraction (EBSD) in a Zeiss ultra 500.

The MO microscope consists of a commercial optical microscope, a helium cryostat with resistive coils and a high quantum efficiency CCD camera [3, 9]. Details of the microscope and the He flow cryostat can be found in [9]. MO imaging is based on the Faraday effect produced by an optically active garnet which is directly laid on the surface of the sample. In our case, the active layer consists of a Fe–Bi doped yttrium iron film grown on a gadolinium gallium garnet (GGG) substrate. Each garnet is characterized by its Verdet constant ( $V$ ), and its optical path ( $d$ ). The local magnetic field is evidenced by a contrast resulting from the polarization rotation  $\theta_f = V * H_{ext} * d$ . The MO was performed at 55mT in field cooled (FC) because this procedure highlights all the defects, compared to zero field cooled (ZFC). The flux is trapped at high temperature ( $\approx 90$  K) where the YBCO grains are poorly coupled and the superconducting layer is more sensitive to the defects. Two Helmholtz coils are fixed on the cryostat and can apply a maximum magnetic field of  $100 \pm 0.2$  mT. The temperature range of observation is 6–300 K. The optical parts, especially the polarizer and analyzer, have been chosen in order to minimize depolarizing effects.

### III. RESULTS

The performance of the LZO buffer layers was evaluated by depositing 450 to 800 nm thick YBCO layers by MOCVD on these films. No NiO was produced during YBCO depositions as deduced by XRD [5]. This experiment confirmed that an 80 nm thick LZO layer was thick enough to ensure a good protection against oxygen diffusion for the MOCVD process.

The textures of YBCO and LZO films were quantified by XRD and EBSD [5]. XRD analyses confirmed the biaxial texture of both layers. Taking into account XRD and EBSD results, it is obvious that the microstructure of YBCO film is directly linked to the crystalline of both substrate and buffer layer. Accordingly to EBSD study, the growth of LZO and YBCO are strongly influenced by the underlying NiW grains. The Fig. 1 shows clearly that the microstructure of NiW substrate is transferred to LZO and then to YBCO films [5]. Defects like grain boundaries or rolling scratches are also transmitted to the different layers, Fig. 1. However, LZO layer has a smoothing effect on the NiW grain boundaries and affords an improved percolation path (most of the grain boundaries have angles smaller than  $7^\circ$ , represented as green and yellow lines in Fig. 1). As most of the grain boundaries

are inferior to  $7^\circ$  in the LZO and YBCO layers, the underlying NiW grain boundaries shouldn't strongly affect current percolation in the YBCO layer.

Optics and MO observations have been realized on NiW/LZO/YBCO samples. Measurements were performed in FC to highlight the defects of the YBCO film, Fig. 2. It appears clearly that vortices are trapped along YBCO grain boundaries which are transferred from NiW grain boundaries. The trapped field highlights bad connections between YBCO grains due to misorientation angle between adjacent NiW grains. Such typical patterns were already observed by Feldmann et al. and Van Der Laan et al. in Ni<sub>RABiTS</sub> based coated conductors [10-12]. This study points out once more that the YBCO quality is directly linked to the substrate microstructure.

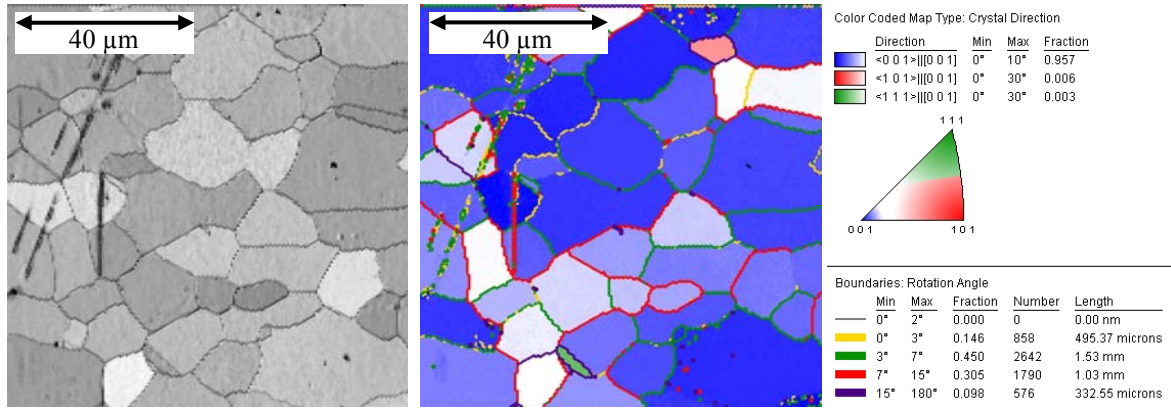
However, it is important to notice that the critical current of the observed sample in Fig. 2 is  $0.8 \text{ MA.cm}^{-2}$  at 77 K in self field despite the bad coupling of some YBCO grains along NiW grain boundaries which can be observed with a 56 mT external field at 20K. This means that the current can percolate even if the connectivity between YBCO grains is not perfect.

The influence of LZO thickness on YBCO properties was also studied. The biaxial texture of the YBCO layers was determined by XRD when increasing LZO thickness, (Fig. 3.a). The average misorientation angle tends to rise up when the thickness of the buffer layer is increased. This behavior is linked to the variation in texture of the LZO layer when increasing its thickness. This loss of texture is presumed to be at the origin of the loss of critical current in YBCO films.

$J_c$  measurement on LZO-buffered Ni were normalized with  $J_c$  values obtained on LAO in the same run in order to discriminate the effect of the thickness from the other deposition conditions; in these conditions  $J_{c,LAO} \approx 0,6 \text{ MA.cm}^{-2}$ . The normalized  $J_c$  value points out that  $J_c$  is unexpectedly increased for thicker LZO films, Fig. 3.b.

This increase of  $J_c$  can be explained by the smoothing effect of LZO layer on NiW grain boundaries, as previously explained. NiW/LZO/YBCO samples with different LZO thicknesses have been observed to visualize its influence on YBCO film quality, Fig. 4. The samples were cooled down in FC until 12 K at 55 mT. Pictures contrast was enhanced to better visualize the defects. When LZO thickness is inferior to 80-100 nm, all the defects of the substrates are transferred to the YBCO film: the vortexes are trapped over NiW grain boundaries and also over rolling scratches caused by the RABiTS process. When the thickness is increased over 150 nm, most of the defects are absorbed by the buffer layer and the percolation path in YBCO film is highly improved. This explains the increase of  $J_c$  despite the degradation of texture of the YBCO film when increasing LZO thickness.

a) NiW



b) LZO

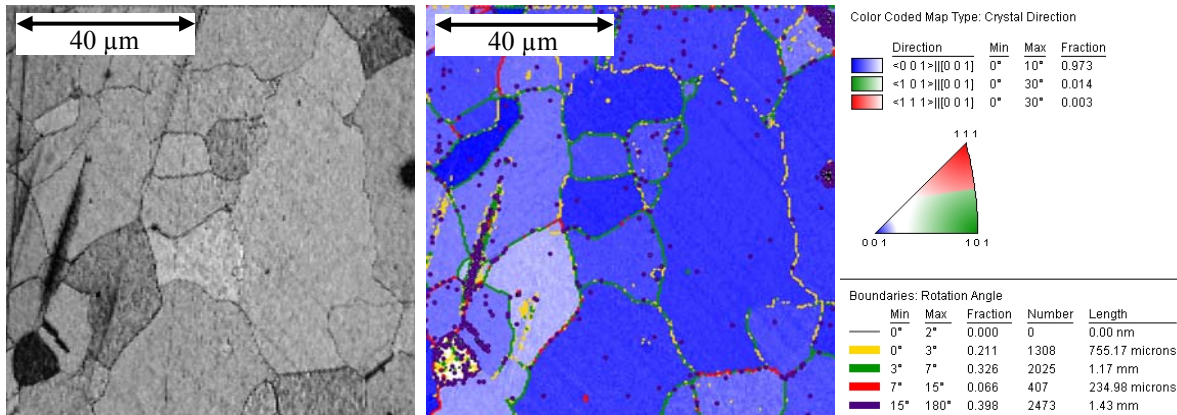


Fig. 1. Images quality and EBSD maps of the NiW (a) and LZO (b) layers used to grow NiW<sub>RABITS</sub>/LZO<sub>MOD</sub>/YBCO<sub>MOCVD</sub> architecture. The images were not taken at the same location, but are representative of the whole sample. The triangles represent the inverted pole figures showing the three main orientations of the crystallites displayed in three different color gradients in the EBSD map. The desired orientation [001] was arbitrary represented in blue. The color gradient represents the out-of-plane disorientation angle of a specific grain with respect to the normal of the sample [001].

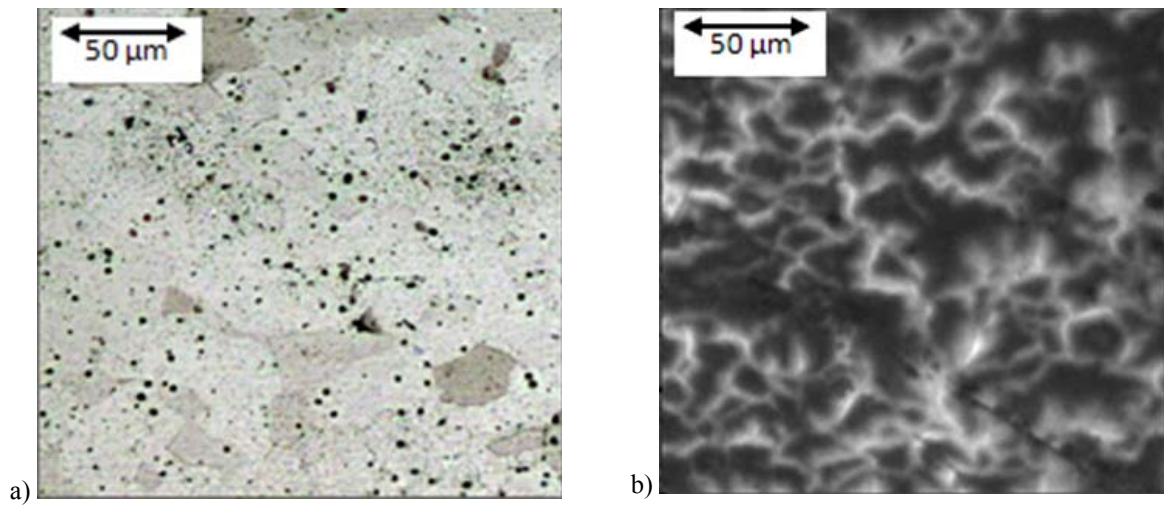


Fig. 2. Optical microscope image under polarized light (a) and MO image (b) of a NiW/LZO<sub>80nm</sub>/YBCO<sub>600nm</sub> coated conductor obtained at 15 K in FC at 55 mT. The magnetic field penetrated along the grain boundaries revealed in the optical image.

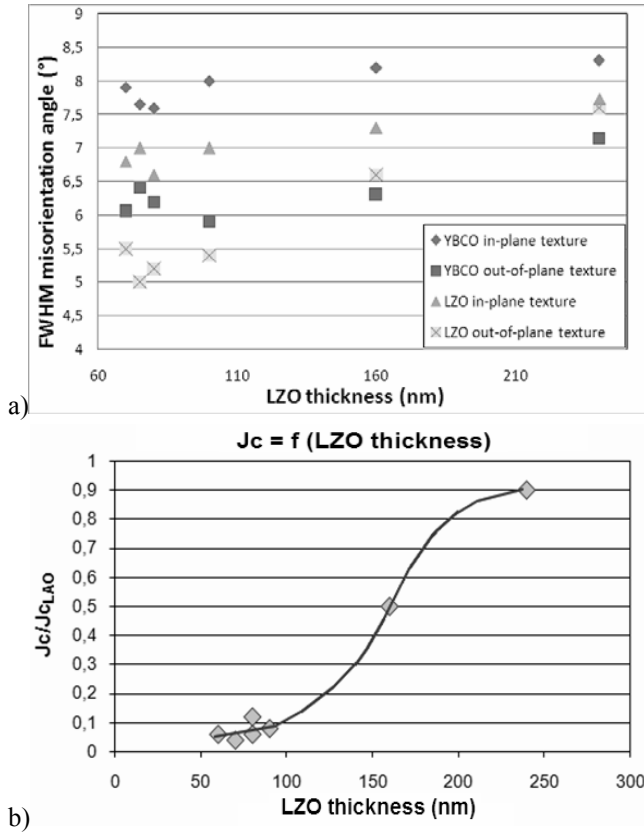


Fig. 3. Influence of the LZO thickness on (a) LZO and YBCO textures and (b) current density of the YBCO film versus LZO thickness

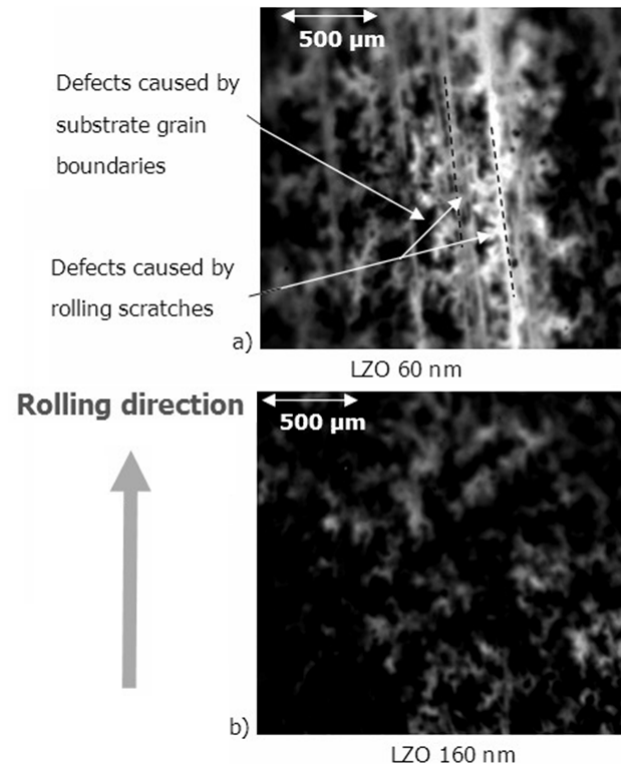


Fig. 4. MO images of YBCO films deposited on  $Ni_{RABITS}$  covered by LZO with different thickness (a) 60 nm and (b) 160 nm: the samples were cooled down in FC until 12 K - 55 mT. Contrast was increased to have a better visualization of the defects.

This points out the necessity to deposit thick LZO buffer layers to smooth the defects of the substrate and ensure higher  $J_c$ . It is very interesting to notice that even if the texture quality becomes worse, the thickness provides a sufficient percolation path to overcome the degradation induced by the surface of the substrate. In such  $Ni_{RABITS}$  based conductor, the microstructure of the substrate and the buffer layer is the most influent factor on current percolation and thus on  $J_c$ .

## I. CONCLUSION

MO combined to EBSD has been used to characterize the microstructure of YBCO films deposited on NiW substrates. The EBSD enables to image the microstructure of the YBCO film. EBSD observations were correlated with MO studies: the magnetic field penetrates through the weakest connections in the YBCO film, and it appears that they are linked with the grain boundaries of the substrate.

The critical current is limited by these grain boundaries. Increasing the thickness of the buffer layer enables to erase these defects as well as larger scratches present on the substrate after rolling. It is suggested that the increase of the thickness smoothes the grooves and decreased the local misalignments in the YBCO film even if the average texture is less sharp. The thickness of the buffer layer is an important parameter to optimize superconducting performance of RABITS based CCs.

Using an appropriate LZO thickness to ensure a sufficient texture quality and absorb most of the defects of the substrate ( $150 \text{ nm} > LZO_{\text{thickness}} > 250 \text{ nm}$ ), it is possible to develop efficient simple low cost coated conductors such as NiW/LZO/YBCO.

## REFERENCES

- [1] Jooss C, Albrecht J, Kuhn H, Leonhardt S and Kronmüller H 2002 Rep. Prog. Phys. 65 651
- [2] Wijngaarden R J, Surdeau R, Griessen R, Menovsky A A, Fendrich J and Kwok W K 1997 Physica C 282–287 2291
- [3] Laviano F, Botta D, Chiodoni A, Gerbaldo R, Ghigo G, Gozzelino L, Zanella S and Mezzeti E 2003 Supercond. Sci. Technol. 16 71
- [4] A Villaume, L Porcar, D Bourgault, A Antonevici, T Caroff, J P Leggeri and C Villard, Supercond. Sci. Technol. 21 (2008) 034009 (6pp)
- [5] T. Caroff, S Morlens, A Abrutis, M Decroux, P Chaudouët, L Porcar, Z Saltyte, C Jiménez, P.Odier and F Weiss. Supercond. Sci. Technol. 21 (2008) 075007.
- [6] J.W. Seo, J. Fompeyrine, A. Guiller, G. Norga, C. Marchiori, H. Siegwart, J.P. Locquet. Appl Phys Lett 83, NO 25, 5211-5213
- [7] Soubeyroux J L, Bruzek C E, Girard A and Jorda J L 2005 IEEE Trans. Appl. Supercond. 15 2687–90
- [8] S. Morlens, Z. M. Yu, N. Marcellin, T. Caroff et al., Chem. Mater. Cm-2008-01668e
- [9] Villaume A, Antonevici A, Bourgault D, Porcar L, Leggeri J P and Villard C 2007 Supercond. Sci. Technol. 20 1019
- [10] Feldmann D M et al 2001 IEEE Trans. Appl. Supercond. 11 3772–5
- [11] Feldmann D M et al 2000 Appl. Phys. Lett. 77 2906
- [12] Van Der Laan D C, Dhalle M, Van Eck H J N, Metz A, Ten Haken B, Ten Kate H H J, Naveira L M, Davidson M W and Schwartz J 2005 Appl. Phys. Lett. 3 32512